

2012

A Computationally Efficient Hybrid Leakage Model for Modeling Leakage in Positive Displacement Compressors

Ian H. Bell
ian.h.bell@gmail.com

Eckhard A. Groll

James E. Braun

W. Travis Horton

Follow this and additional works at: <http://docs.lib.purdue.edu/icec>

Bell, Ian H.; Groll, Eckhard A.; Braun, James E.; and Horton, W. Travis, "A Computationally Efficient Hybrid Leakage Model for Modeling Leakage in Positive Displacement Compressors" (2012). *International Compressor Engineering Conference*. Paper 2038. <http://docs.lib.purdue.edu/icec/2038>

This document has been made available through Purdue e-Pubs, a service of the Purdue University Libraries. Please contact epubs@purdue.edu for additional information.

Complete proceedings may be acquired in print and on CD-ROM directly from the Ray W. Herrick Laboratories at <https://engineering.purdue.edu/Herrick/Events/orderlit.html>

A Computationally Efficient Hybrid Leakage Model for Modeling Leakage in Positive Displacement Compressors

Ian H. BELL^{1*}, Eckhard A. GROLL², James E. BRAUN², W. Travis HORTON²

¹Bell Thermal Consultants
ian.h.bell@gmail.com

²Purdue University, Mechanical Engineering Department, Herrick Labs
West Lafayette, IN, USA
eagroll@purdue.edu, jbraun@purdue.edu, wthorton@purdue.edu

* Corresponding Author

ABSTRACT

An empirical frictional correction factor to the isentropic nozzle model has been developed for application to leakage modeling in scroll, rotary and other similar compressors. This correction factor is derived by calculating the leakage mass flow with a compressible, variable area, real gas properties model and then correlating the ratio of this flow to the isentropic nozzle model prediction. The ratio of flows is correlated to the Reynolds number, a characteristic length and the leakage gap width. A representative selection of fluids and geometries are employed, and the correlations predict at least 93% of the detailed model results within an absolute error band of 20%.

1. INTRODUCTION

One of the most challenging elements of the modeling involved in positive-displacement compressors is the modeling of leakage. The modeling of leakage flows in compressors is particularly difficult since in most cases the leakage gap widths are not known *a priori*, and the leakage flow is in general compressible, frictional, and the flow area changes over the length of the flow path. As a result, the use of simple models like the isentropic nozzle model for leakage flow results in large discrepancies when compared with more accurate detailed leakage flow modeling. The more detailed models can capture all the physical effects simultaneously, but require a great deal of computational effort, precluding their implementation in more detailed compressor models.

In this paper, a hybrid method is proposed whereby the results from a detailed leakage flow calculations are used to derive a simple correction term to the isentropic nozzle model. In this way, the computational efficiency of the isentropic nozzle model can be retained, with only a slight loss in accuracy of prediction of the leakage flow rates under choked conditions.

The models are developed based on the scroll compressor geometry, but their formulation can be applied to any leakage flow calculation.

2. LITERATURE REVIEW

The typical baseline model for leakage in scroll compressors is the compressible flow of a perfect gas through an isentropic adiabatic converging nozzle. This model allows for choking when the Mach number reaches 1 at the throat. This model is typically used with empirical correction factors to compensate for static pressure losses in the flow path. This is the model of choice for a number of authors, including Margolis (1992), Puff (1992), Youn (2000), Lee (2002), Chen (2002), among many others. The primary motivating factor for the use of this model is its simplistic form as only one area, the throat area, is required. In addition the mass flow is explicitly obtained from the compressible mass flow expression, adding little computational overhead if implemented into a detailed model. Typically this model is applied to both flank and radial leakages. One of the challenges is the determination of the discharge coefficient, and limited experimental data is available, but Cho et al. (2000) have investigated this problem and found a discharge coefficient of 0.1 fit their choked flow data well, which suggests that the isentropic

flow model does not do a very good job of capturing the actual leakage mass flow rate since such a large correction is required.

One of the major shortcomings of the isentropic compressible flow model is that it does not take friction into account. However, the leakage paths are relatively long relative to the leakage gap widths. In a typical scroll compressor, the lengths of the leakage flow paths can be up to 500 times as long as the gaps are wide. Therefore friction can be expected to play a significant role in the flow through the leakages.

Frictional flow models can be categorized based on their treatment of compressibility; some models treat the fluid as incompressible, others as compressible. For incompressible flow, the pressure drop over the leakage path can be calculated from incompressible pipe flow relations, as suggested by Ishii (1996). Very good agreement is found with experimental measurements carried out on a specialized test stand built to test leakage characteristics. Yuan (1992) and Fan (1994) extend the incompressible flow with friction model to account for the inertial terms in the Navier-Stokes equations which are neglected in the pipe flow analysis but end up at an expression which needs to be integrated over the flow path. They find that their model provides results that are superior to that of either isentropic compressible nozzle flow or to pipe flow. Kang (2002) found that using compressible adiabatic flow with friction (Fanno Flow) was a good match to the predictions of FLUENT results, and superior to the use of isentropic compressible nozzle flow. Suefuji (1992) also found good results by using Fanno flow through the leakages.

Li presents a model for the radial leakage flow based on the flow between cylinders (1992), but is missing units, while Yanagisawa (1985) presents the same model with the necessary description and units. Tseng (2006) also uses the same model.

Beyond the simplified models, there are a number of hybrid models that select elements from several models. Tojo (1986) used a combined converging isentropic nozzle/compressible frictional flow section to model the flow through the leakages. Afjei (1992) used superposition methods to calculate the volumetric flow through the leakages as a sum of the rolling, dragging, pressure driven, and flashing components.

The primary disadvantage of the detailed models is that while they can accurately predict the mass flow rate through the leakage gaps, they are extremely computationally expensive. As a result, they cannot be practically employed in detailed compressor models. This is the motivation for the use of a frictional correction term to the isentropic nozzle model.

3. DETAILED MODEL DEVELOPMENT

In this section, the analysis required for the detailed model is developed. The analysis presented here largely follows that from the analysis of Wassgren (2009), but modifications are made for the addition of changing area and real gas properties. In the analysis that follows, the following assumptions have been employed:

- No heat transfer
- No mass transfer
- Variable area
- Compressible flow
- Real gas properties
- One-dimensional flow

3.1 Continuity

The mass flow through the differential area can be given by

$$\dot{m} = \rho VA \quad (1)$$

which is constant since there is no mass addition or subtraction. Thus taking the derivative of the mass flow rate with respect to the flow direction and setting it equal to zero yields

$$\frac{1}{\rho} \frac{d\rho}{dx} + \frac{1}{V} \frac{dV}{dx} + \frac{1}{A} \frac{dA}{dx} = 0 \quad (2)$$

3.2 Momentum

Conservation of momentum for the control volume is given by

$$\int_{CS} \rho V^2 dA = \sum F \quad (3)$$

which yields

$$\rho V \frac{dV}{dx} + \frac{dp}{dx} = -\frac{\rho V^2}{2} \frac{4f_F}{D_H} \quad (4)$$

when products of differentials are dropped. The Fanning friction factor is given by

$$f_F = \begin{cases} \frac{24}{\text{Re}} & \text{Re} < 1736.5 \\ \frac{(0.790 \ln \text{Re} - 1.64)^{-2}}{4} & \text{Re} > 1736.5 \end{cases} \quad (5)$$

which assumes a model for flow between infinite plates is reasonable. In the transitional Reynolds number regime, the turbulent and laminar Reynolds number curves are extrapolated to intersection at a Reynolds number of 1763.5 in order to ensure that the friction factor curve is monotonic, aiding numerical convergence. The local Reynolds number is based on the local hydraulic diameter of the flow path, and is defined below for each flow path.

3.3 Energy

Since the differential element is treated as carrying out no boundary work or heat transfer with its surroundings, the stagnation enthalpy is constant, thus the conservation of energy is given by

$$\dot{m} \left(h + \frac{V^2}{2} \right) - \dot{m} \left(h + dh + \frac{(V + dV)^2}{2} \right) = 0 \quad (6)$$

which reduces to

$$\frac{dh}{dx} + V \frac{dV}{dx} = 0 \quad (7)$$

when the products of differentials are dropped.

3.4 Thermodynamic Properties and partial derivatives

In order to use the real gas properties of the refrigerant, the pressure and enthalpy need to be expanded in terms of T and ρ . For a single-phase fluid, two state variables are needed to fix the state of the fluid, and the reference equations of state for most common fluids are expressed as a function of temperature and density. Thus the partial derivatives of enthalpy and pressure can be explicitly obtained from the equation of state formulation. The differential of enthalpy is given by

$$dh = \frac{\partial h}{\partial T} dT + \frac{\partial h}{\partial \rho} d\rho \quad (8)$$

$$dp = \frac{\partial p}{\partial T} dT + \frac{\partial p}{\partial \rho} d\rho \quad (9)$$

and dividing through by dx yields

$$\frac{dh}{dx} = \frac{\partial h}{\partial T} \frac{dT}{dx} + \frac{\partial h}{\partial \rho} \frac{d\rho}{dx} \quad (10)$$

$$\frac{dp}{dx} = \frac{\partial p}{\partial T} \frac{dT}{dx} + \frac{\partial p}{\partial \rho} \frac{d\rho}{dx} \quad (11)$$

The residual Helmholtz energy formulation of the properties gives the pressure and enthalpy in the forms

$$\frac{p}{\rho RT} = 1 + \delta \left(\frac{\partial \alpha^r}{\partial \delta} \right)_\tau \quad (12)$$

$$\frac{h}{RT} = \tau \left[\left(\frac{\partial \alpha^0}{\partial \tau} \right)_\delta + \left(\frac{\partial \alpha^r}{\partial \tau} \right)_\delta \right] + \delta \left(\frac{\partial \alpha^r}{\partial \delta} \right)_\tau + 1 \quad (13)$$

where $\tau = T_c/T$ and $\delta = \rho/\rho_c$, and T_c and ρ_c are the critical temperature and density of the fluid respectively. All of the fluid equations of state employed here (Span, 1996; Span, 2000; Lemmon, 2003; Tillner-Roth, 1994) are of the residual Helmholtz energy formulation. Both the ideal gas Helmholtz energy contribution (α_0) and residual

Helmholtz energy contribution (α_r) are in general functions of temperature and density. Lemmon (2000) gives the necessary partial derivatives of the pressure directly:

$$\frac{\partial p}{\partial \rho} = RT \left[1 + 2\delta \left(\frac{\partial \alpha^r}{\partial \delta} \right)_\tau + \delta^2 \left(\frac{\partial^2 \alpha^r}{\partial \delta^2} \right)_\tau \right] \quad (14)$$

$$\frac{\partial p}{\partial T} = R\rho \left[1 + \delta \left(\frac{\partial \alpha^r}{\partial \delta} \right)_\tau - \delta\tau \left(\frac{\partial^2 \alpha^r}{\partial \delta \partial \tau} \right)_\tau \right] \quad (15)$$

Calculations for partial derivatives of the enthalpy are straightforward, and given by the terms

$$\frac{\partial h}{\partial \rho} = \frac{RT}{\rho_c} \left\{ \tau \left[\left(\frac{\partial^2 \alpha^0}{\partial \tau \partial \delta} \right)_\delta + \left(\frac{\partial^2 \alpha^r}{\partial \tau \partial \delta} \right)_\delta \right] + \left(\frac{\partial \alpha^r}{\partial \delta} \right)_\tau + \delta \left(\frac{\partial^2 \alpha^r}{\partial \delta^2} \right)_\tau \right\} \quad (16)$$

$$\frac{\partial h}{\partial T} = \frac{1}{\rho} \left(\frac{\partial p}{\partial T} \right)_\rho - R\tau^2 \left[\left(\frac{\partial^2 \alpha^0}{\partial \tau^2} \right)_\delta + \left(\frac{\partial^2 \alpha^r}{\partial \tau^2} \right)_\delta \right] \quad (17)$$

3.5 Solution for System of ODE

With the use of a computer algebra system (Maxima), the derivatives of each of the variables can be obtained and the solution for the system of differential equations is obtained as given by Equations (18) to (22) seen below. With this model, in order to calculate the flow rate through a leakage gap width, the flow area as a function of x is needed. With the flow area then known, it is possible to numerically integrate these derivatives from the inlet of the flow path to the outlet of the flow path. The improved Euler method (also known as Heun's method or the Euler-Cauchy method) is used to integrate the system of equations along the flow path.

The problem for the calculation of the flow for a given leakage path is formulated with the upstream temperature, upstream pressure, and downstream pressure specified as known. The problem then is to find the mass flow rate that yields the downstream pressure at the outlet of the flow path. If the final pressure from the integration is equal to the downstream pressure, the mass flow rate has been appropriately calculated. The flow is constrained to be sub-sonic; that is, there are no normal shocks or choking in the flow path. The mass flow rate predicted by the detailed compressible flow model is given by \dot{m}_d .

$$\frac{dT}{dx} = - \frac{2\rho A f_F V^4 + \left(\frac{dA}{dx} \left(\frac{\partial p}{\partial \rho} \rho D_H - \frac{\partial h}{\partial \rho} \rho^2 D_H \right) - 2 \frac{\partial h}{\partial \rho} \rho^2 A f_F \right) V^2}{A \left(\rho D_H \frac{\partial h}{\partial T} - D_H \frac{\partial p}{\partial T} \right) V^2 + \rho A D_H \left(\frac{\partial h}{\partial \rho} \frac{\partial p}{\partial T} - \frac{\partial p}{\partial \rho} \frac{\partial h}{\partial T} \right)} \quad (18)$$

$$\frac{dp}{dx} = - \frac{2\rho A \frac{\partial p}{\partial T} f_F V^4 + \rho^2 \left(2A f_F + \frac{dA}{dx} D_H \right) \left(\frac{\partial p}{\partial \rho} \frac{\partial h}{\partial T} - \frac{\partial h}{\partial \rho} \frac{\partial p}{\partial T} \right) V^2}{A \left(\rho D_H \frac{\partial h}{\partial T} - D_H \frac{\partial p}{\partial T} \right) V^2 + \rho A D_H \left(\frac{\partial h}{\partial \rho} \frac{\partial p}{\partial T} - \frac{\partial p}{\partial \rho} \frac{\partial h}{\partial T} \right)} \quad (19)$$

$$\frac{d\rho}{dx} = - \frac{\left(2\rho^2 A \frac{\partial h}{\partial T} f_F + \frac{dA}{dx} \left(\rho^2 D_H \frac{\partial h}{\partial T} - \rho D_H \frac{\partial p}{\partial T} \right) \right) V^2}{A \left(\rho D_H \frac{\partial h}{\partial T} - D_H \frac{\partial p}{\partial T} \right) V^2 + \rho A D_H \left(\frac{\partial h}{\partial \rho} \frac{\partial p}{\partial T} - \frac{\partial p}{\partial \rho} \frac{\partial h}{\partial T} \right)} \quad (20)$$

$$\frac{dh}{dx} = - \frac{2\rho A \frac{\partial h}{\partial T} f_F V^4 + \rho \frac{dA}{dx} D_H \left(\frac{\partial p}{\partial \rho} \frac{\partial h}{\partial T} - \frac{\partial h}{\partial \rho} \frac{\partial p}{\partial T} \right) V^2}{A \left(\rho D_H \frac{\partial h}{\partial T} - D_H \frac{\partial p}{\partial T} \right) V^2 + \rho A D_H \left(\frac{\partial h}{\partial \rho} \frac{\partial p}{\partial T} - \frac{\partial p}{\partial \rho} \frac{\partial h}{\partial T} \right)} \quad (21)$$

$$\frac{dV}{dx} = \frac{2\rho A \frac{\partial h}{\partial T} f_f V^3 + \rho \frac{dA}{dx} D_H \left(\frac{\partial p}{\partial \rho} \frac{\partial h}{\partial T} - \frac{\partial h}{\partial \rho} \frac{\partial p}{\partial T} \right) V}{A \left(\rho D_H \frac{\partial h}{\partial T} - D_H \frac{\partial p}{\partial T} \right) V^2 + \rho A D_H \left(\frac{\partial h}{\partial \rho} \frac{\partial p}{\partial T} - \frac{\partial p}{\partial \rho} \frac{\partial h}{\partial T} \right)} \quad (22)$$

4. ISENTROPIC NOZZLE FLOW

For the isentropic compressible nozzle flow model, the upstream and downstream pressures and the throat area are given. This model assumes that the fluid is an ideal gas with compressibility taken into account, but there is no friction. If the imposed pressure ratio is large enough to obtain sonic conditions at the throat of the nozzle, the flow is choked. The critical pressure ratio that yields sonic conditions at the throat of the nozzle is given by

$$p_{r,c} = \left(1 + \frac{k-1}{2} \right)^{k/(1-k)} \quad (23)$$

where k is the ratio of specific heats, given by $k=c_p/c_v$, evaluated at the upstream condition. The pressure ratio employed in the isentropic nozzle model is given by

$$p_r = \begin{cases} p_{r,c} & p_{down} / p_{up} \leq p_{r,c} \\ p_{down} / p_{up} & p_{down} / p_{up} > p_{r,c} \end{cases} \quad (24)$$

Thus the mass flow rate from the isentropic nozzle model is given by

$$\dot{m}_n = A_n \sqrt{p_{up} \rho_{up}} \sqrt{\frac{2k}{k-1} \left(p_r^{2/k} - p_r^{(k+1)/k} \right)} \quad (25)$$

where A_n is the nozzle throat area, defined based on the geometry as shown below. For a given configuration, the ratio of the isentropic nozzle mass flow rate prediction to that of the detailed model is defined by

$$M \equiv \frac{\dot{m}_n}{\dot{m}_d} \quad (26)$$

5. LEAKAGE PATH GEOMETRY

The analysis that follows in this section is primarily focused on the geometry of the scroll compressor as it has the most challenging geometric features to model. However, the resulting empirical correlations can be applied to other styles of compressors with minimal modification.

5.1 Scroll Compressor Radial Leakage

Figure 1 shows the geometry of the simplified radial leakage path of the scroll compressor. The flow goes from a high pressure volume out to a lower pressure volume through an annulus with inner radius r_1 and outer radius r_2 with height δ . In practice, the geometry of the scroll compressor is not exactly like that of the simplified geometry, but it is at least locally. For application of the correlation in a detailed compressor model, average radii of curvature can be used in the place of r_1 and r_2 .

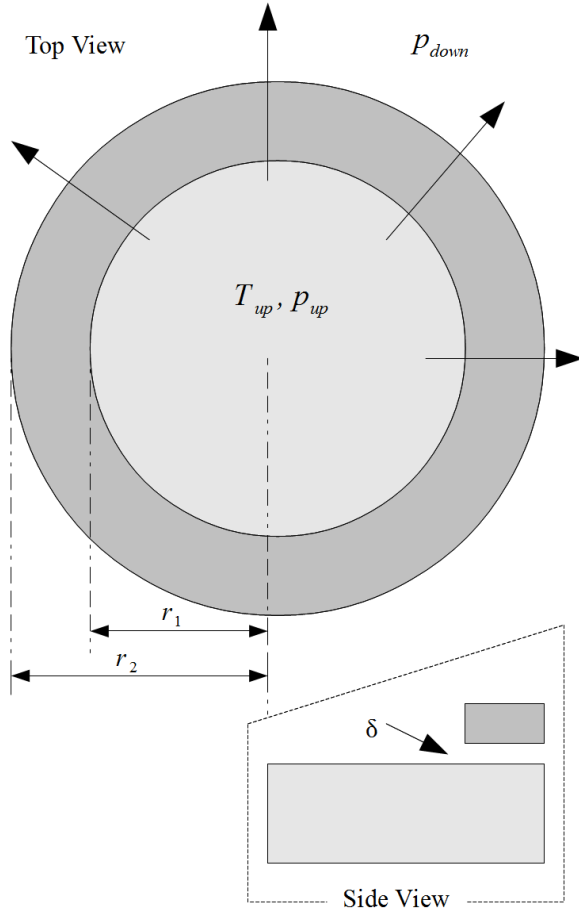


Figure 1: Radial leakage geometry schematic

The cross-sectional area at a position x is equal to

$$A = 2\pi\delta x \quad (27)$$

where x goes from r_1 to r_2 . The derivative of A is given by

$$\frac{dA}{dx} = 2\pi\delta \quad (28)$$

and the area used in the isentropic nozzle model is given by

$$A_n = 2\pi\delta r_1 \quad (29)$$

The Reynolds number is based on the upstream geometry and is given by

$$\text{Re}_n = \frac{\dot{m}_n}{\pi r_1 \mu} \quad (30)$$

where the viscosity μ is evaluated at the upstream state. For the radial leakage, the characteristic length L in the correlation is equal to $L=r_2-r_1$, which for a scroll compressor is simply equal to the scroll wrap thickness. The hydraulic diameter is given by $D_H=2\delta$

5.2 Scroll Compressor Flank Leakage

The flow through the flank leakage is flow through a converging-diverging nozzle formed by the conformal contact of the outer surface of one scroll wrap and the inner surface of the mating scroll wrap. The area of the flank flow path is given as a function of sweep angle ϕ (Yanagisawa, 1985) as

$$A = h \left[R - (R - r - \delta) \cos \phi - \sqrt{r^2 - (R - r - \delta)^2 \sin^2 \phi} \right] \quad (31)$$

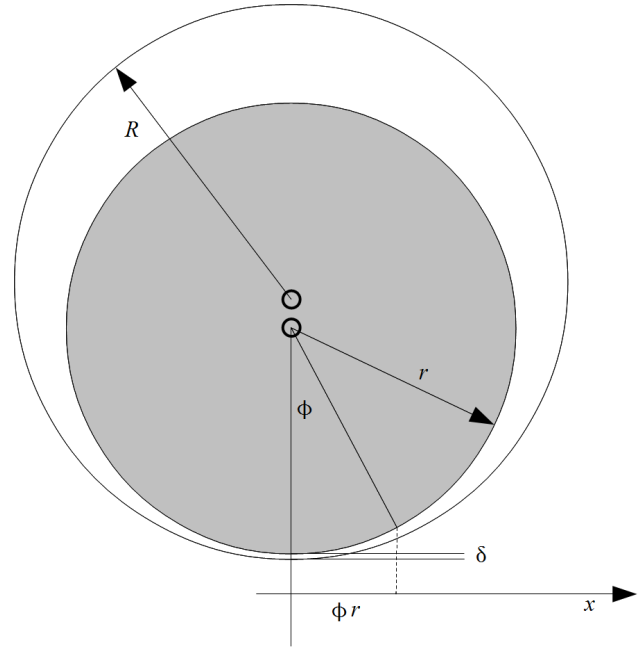


Figure 2: Flank leakage geometry schematic

where δ is the minimum gap width, h is the height out of the page and r and R are the radii of the inner and outer cylinders respectively. The x -coordinate corresponding to an angle ϕ is given by $x=\phi r$, the sweep angle for evaluation of the area can be obtained from $\phi=x/r$. Thus the derivative of the area with respect to x is

$$\frac{dA}{dx} = \frac{h}{r} \left[(R-r-\delta) \sin \phi + \frac{(R-r-\delta)^2 \sin \phi \cos \phi}{\sqrt{r^2 - (R-r-\delta)^2 \sin^2 \phi}} \right] \quad (32)$$

For the flank leakage, the characteristic length L is taken to be equal to $L=R-r$ which simple algebra shows is equal to the orbiting radius r_o for the scroll compressor. The characteristic area for the isentropic nozzle model is equal to the minimum area of the flow path, or

$$A_n = \delta h \quad (33)$$

where h is the height out of the page. The Reynolds number for the flank leakage flow is equal to

$$\text{Re}_n = \frac{2\dot{m}_n}{h\mu} \quad (34)$$

where the viscosity μ is evaluated at the upstream state.

6. DEVELOPMENT OF CORRELATION

The detailed model and the isentropic nozzle model were evaluated for a range of conditions for a range of working fluids and both the flank and radial leakages. The same geometry (that of the compressor of Bell (2011)) was used for a range of fluids, detailed in Table 1. For each refrigerant, the high-side pressure was varied through the range shown, and then for each upstream pressure, the downstream pressure was decreased until a pressure ratio of $p_{r,max}$ was reached. The gap width was varied in the range 5 μm to 25 μm . The results of these runs of the models form a database of two sets of data using the detailed and isentropic nozzle models. The ratio of the mass flow predictions is then the correction factor M that is desired.

Table 1: Refrigerant states for development of frictional correction factor

Refrigerant	p_{up} [kPa]	$p_{r,max}$ [-]	T_{up} [K]
Nitrogen	1800-400	1.5	320
CO ₂	8000-6000	1.5	320
R134a	1500-400	1.5	350
R410A	1500-1000	1.5	350

Figure 3 and Figure 4 show the results of the dataset generated. Both the radial and flank flow paths exhibit similar behaviors. The larger M is, the more important the frictional effects are. If M is 100, the isentropic nozzle gives a prediction of the mass flow rate that is 100 times too high because the isentropic nozzle model neglects frictional effects. The frictional effects become more important at lower Reynolds numbers. For both flank and radial leakages, as the gap width goes down or the characteristic length increases, the frictional effects increase and the value of M increases.

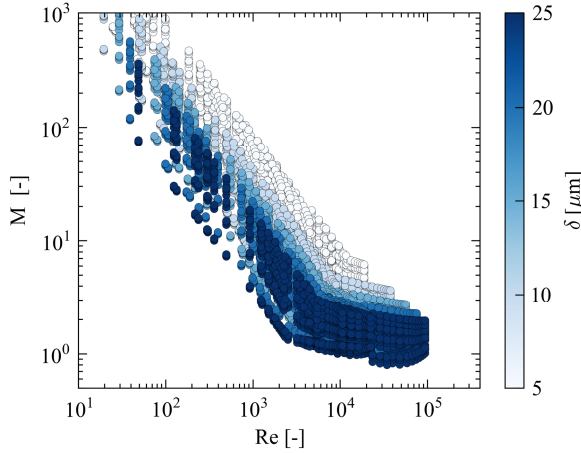


Figure 3: Ratio of isentropic nozzle model to detailed model for radial leakage as a function of Re and δ

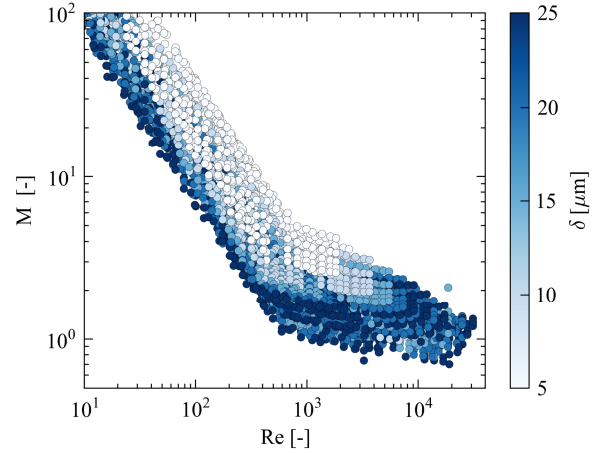


Figure 4: Ratio of isentropic nozzle model to detailed model for flank leakage as a function of Re and δ

7. DEVELOPED CORRELATION

Once the dataset of mass flow predictions has been developed for each flow path, it is then necessary to develop a correlation to obtain the detailed mass flow predictions as a function of the nozzle model mass flow predictions. A number of functional forms of the correlation have been investigated, but the following form was obtained through regression and minimization of the root-mean-squared error of the correlation. The form of the correlation obtained is

$$M = \frac{a_0 (L^*)^{a_1}}{a_2 (\delta^*) + a_3} [\xi (a_4 \text{Re}_n^{a_5} + a_6) + (1 - \xi)(a_7 \text{Re}_n^{a_8} + a_9)] + a_{10} \quad (35)$$

where the cross-over term ξ is given by

$$\xi = \frac{1}{1 + \exp[-0.01(\text{Re} - \text{Re}^*)]} \quad (36)$$

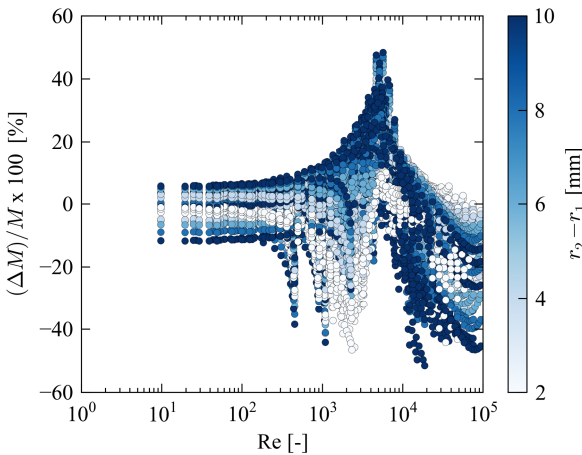
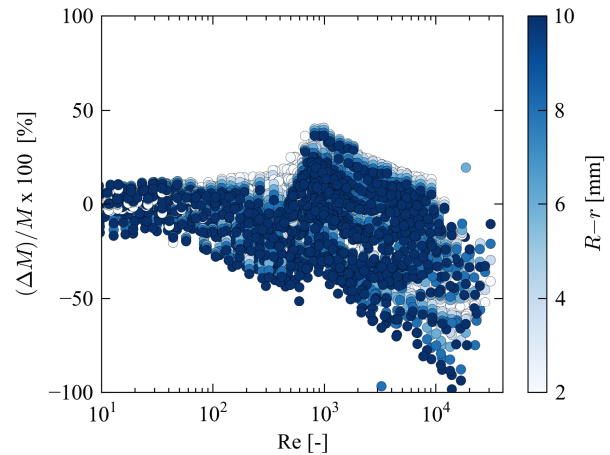
which is used to allow the curve fit optimizer to obtain two separate and continuous solutions for the low- and high-Reynolds numbers portions. The non-dimensionalized characteristic length and non-dimensionalized gap width are given by $L^* = L/L_0$ and $\delta^* = \delta/\delta_0$, where the non-dimensionalization parameters are given by $L_0 = 0.005$ m and $\delta_0 = 10 \times 10^{-6}$ m. The same non-dimensionalization parameters are used for both the flank and radial paths. The coefficients for the radial and flank flow paths are found in Table 2 and Table 3 respectively. The other terms for the correlations are defined in the respective sections on leakage path geometry. The error in prediction of the radial and flank leakage correlation terms can be found in Figure 5 and Figure 6 respectively. For the radial gap, the worst errors are found near the elbow between low- and high-Reynolds number and at high Reynolds numbers. For the flank gap, the worst errors are found at high Reynolds numbers. For the radial leakages, the average absolute error is 10.79% and the root-mean-squared error in M is 16.36. For the flank leakage, the average absolute error is 14.54% and the root-mean-squared error in the prediction of M is 2.25. For both correlations, at least 93% of the points are predicted within an absolute error band of 20%.

Table 2: Coefficients for empirical correction term for radial leakage gap

Term	Value	Term	Value
a_0	2.59321070e+04	a_6	-1.28861161e-02
a_1	9.14825434e-01	a_7	-1.51202604e+02
a_2	-1.77588568e+02	a_8	-9.99674458e-01
a_3	-2.37052788e-01	a_9	1.61435039e-02
a_4	-1.72347611e+05	a_{10}	8.25533457e-01
a_5	-1.20687600e+01	Re^*	5.24358195e+03

Table 3: Coefficients for empirical correction term for flank leakage gap

Term	Value	Term	Value
a_0	-2.63970396e+00	a_6	-5.10200923e-01
a_1	-5.67164431e-01	a_7	-1.20517483e+03
a_2	8.36554999e-01	a_8	-1.02938914e+00
a_3	8.10567168e-01	a_9	6.89497786e-01
a_4	6.17402826e+03	a_{10}	1.09607735e+00
a_5	-7.60907962e+00	Re^*	8.26167178e+02

**Figure 5: Error in radial correction term as a function of Reynolds Number, gap width, and length****Figure 6: Error in flank correction term as a function of Reynolds Number, gap width, and length**

One of the motivating factors for the hybrid leakage calculation method is to embed the leakage model in a detailed compressor model in order to use the compressor model to predict its performance over a range of operating conditions. For that reason, the detailed model cannot be used directly due to the large amount of iteration needed and the commensurate increase in computational work required. For the flank leakages, using the hybrid method (isentropic nozzle with the correction term) is 1822 times faster than using the detailed model. For the radial leakages, the hybrid method is 40 times faster than the detailed model.

The results for a sample radial leakage for Nitrogen and CO₂ are shown in Figure 7 and Figure 8. The correction term works extremely well for CO₂ since the isentropic nozzle model does not predict choking will occur over the range of back pressures investigated. For nitrogen, the isentropic nozzle model predicts choking will occur, and for those points where choking does occur, the corrected model underpredicts the detailed model. Even so, it is a huge improvement over the use of the isentropic nozzle model.

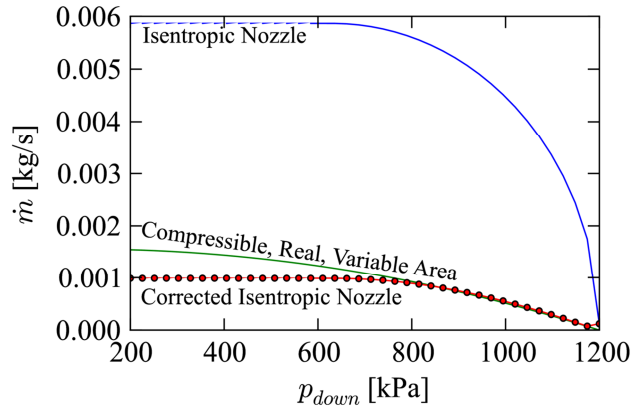


Figure 7: Nitrogen flow rates through the radial gap predicted by isentropic nozzle, detailed models, and corrected isentropic nozzle ($p_{up}=1200$ kPa, $T_{up}=320$ K)

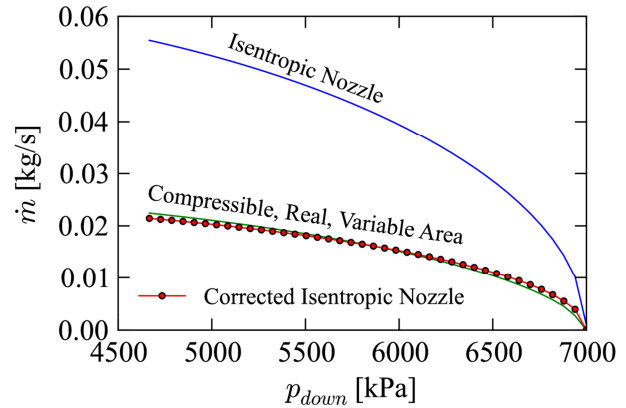


Figure 8: CO₂ flow rates through the radial gap predicted by isentropic nozzle, detailed models, and corrected isentropic nozzle ($p_{up}=7000$ kPa, $T_{up}=320$ K)

7.1 Application to Other Compressor Geometry

The correction terms presented here are most directly applicable to scroll compressors, but they can also be used in other types of compressors. For instance, the flank leakage correction term presented here is of the same form of the leakage around the rotor of rotary-type compressors. In any case, the above methodology can be used to derive a geometrically-appropriate leakage correction term for the compressor of interest.

CONCLUSIONS

With the use of the leakage correction correlation, it is possible to achieve significant improvements in leakage model accuracy compared with the isentropic nozzle model while adding little computational overhead. It is hoped that this model may be broadly used throughout the compressor modeling industry. Further work could be used to improve the model predictions for choked flow.

NOMENCLATURE

a_p, a_1, \dots	-	Correlation coefficients
A	m ²	Area
A_n	m ²	Nozzle throat area
D_H	m	Hydraulic Diameter
f_F	-	Fanning friction factor
F	N	Force
k	-	Ratio of specific heats
L	m	Flow path length
L^*	-	Non-dimen. length
h	J/kg	Enthalpy
\dot{m}	kg/s	Mass flow rate
\dot{m}_d	kg/s	Mass flow rate from detailed
\dot{m}_n	kg/s	Mass flow rate from nozzle
M	-	Ratio of mass flow rates
p	Pa	Pressure
p_{down}	Pa	Downstream pressure
p_{up}	Pa	Upstream pressure

p_r	-	Pressure ratio
$p_{r,c}$	-	Critical pressure ratio
r_1	m ²	Inner radius
r_2	m ²	Outer radius
r	m	Small cylinder radius
R	m	Big cylinder radius
R	J/kg/K	Specific gas constant
Re	-	Reynolds Number
T	K	Temperature
T_{up}	K	Upstream temperature
x	m	Position
V	m/s	Velocity
α^0	-	Ideal-gas Helmholtz
α^r	-	Real-gas Helmholtz
δ	m	Gap width
δ	-	Reduced density
δ^*	-	Non-dimen. gap width

ρ_{up}	kg/m ³	Upstream density
τ	-	Reduced temperature
ϕ	rad	Sweep angle
ξ	-	Cross-over term

ACKNOWLEDGEMENTS

The work in this paper is adapted from the Purdue University PhD. Thesis entitled *Theoretical and Experimental Analysis of Liquid Flooded Compression in Scroll Compressors* by this author, published in 2011. Full-text: <http://docs.lib.purdue.edu/herrick/2/>

REFERENCES

- Afjei, T., Suter, P., Favrat, D., 1992. Experimental analysis of an inverter-driven scroll compressor with liquid injection. In: 1992 Compressor Engineering Conference at Purdue University.
- Bell, I., 2011. *Theoretical and Experimental Analysis of Liquid Flooded Compression in Scroll Compressors*. Ph.D. thesis, Purdue University. Full-text: <http://docs.lib.purdue.edu/herrick/2/>
- Chen, Y., Halm, N., Groll, E., Braun, J., 2002. Mathematical Modeling of Scroll Compressor. Part I- Compression Process Modeling. *International Journal of Refrigeration* 25, 731–750.
- Cho, N.-K., Youn, Y., Lee, B.-C., Min, M.-K., 2000. The Characteristics of Tangential Leakage in Scroll Compressors for Air-conditioners. In: 15th International Compressor Engineering Conference at Purdue University. No. 807-814.
- Fan, Z., Chen, Z., 1994. A calculating method for gas leakage in compressor. In: 1994 Compressor Conference at Purdue University.
- Ishii, N., Bird, K., Sano, K., Oono, M., Iwamura, S., Otokura, T., 1996. Refrigerant Leakage Flow Evaluation for scroll compressors. In: 1996 Compressor Conference at Purdue University.
- Kang, D. J., Kim, J. W., Sohn, C. B., 2002. Effects of leakage flow model on the thermodynamic performance of a scroll compressor. In: 2002 International Compressor Engineering Conference at Purdue University.
- Lee, B.-C., Yanagisawa, T., Fukuta, M., Choi, S., 2002. A study on the leakage characteristics of tip seal mechanism in the scroll compressor. In: 2002 International Compressor Engineering Conference at Purdue University.
- Lemmon, E., 2003. Pseudo-Pure Fluid Equations of State for the Refrigerant Blends R-410A, R-404A, R-507A, and R-407C. *International Journal of Thermophysics* 24 (4), 991–1006.
- Lemmon, E., Jacobsen, R. T., Penoncello, S. G., Friend, D., 2000. Thermodynamic Properties of Air and Mixtures of Nitrogen, Argon, and Oxygen from 60 to 2000 K at Pressures to 2000 MPa. *J. Phys. Chem. Ref. Data* 29 (3), 331–385.
- Li, H., Wang, D., Wang, H., Chen, P., 1992. Research of oil-injected scroll compressor working process. In: 1992 Compressor Engineering Conference at Purdue University. pp. 118b1–118b13.
- Margolis, D. L., Craig, S., Nowakowski, G., Inada, M., 1992. Modeling and simulation of a scroll compressor using bond graphs. In: 1992 International Compressor Engineering Conference at Purdue University.
- Puff, R., Krueger, M., 1992. Influence of the main constructive parameters of a scroll compressor on its efficiency. In: 1992 International Compressor Engineering Conference at Purdue University.
- Span, R., Lemmon, E. W., Jacobsen, R. T., Wagner, W., Yokozeki, A., 2000. A Reference Equation of State for the Thermodynamic Properties of Nitrogen for Temperatures from 63.151 to 1000 K and Pressures to 2200 K. *J. Phys. Chem. Ref. Data* 29, 1361–1433.
- Span, R., Wagner, W., 1996. A New Equation of State for Carbon Dioxide Covering the Fluid Region from the Triple-Point Temperature to 1100 K at Pressures up to 800 MPa. *J. Phys. Chem. Ref. Data* 25, 1509–1596.
- Suefuji, K., Shiibayashi, M., Tojo, K., 1992. Performance analysis of hermetic scroll compressors. In: 1992 International Compressor Engineering Conference at Purdue University.
- Tillner-Roth, R., Baehr, H. D., 1994. A International Standard Formulation for the Thermodynamic Properties of 1,1,1,2-Tetrafluoroethane (HFC-134a) for Temperatures from 170 K to 455 K and Pressures up to 70 MPa. *J. Phys. Chem. Ref. Data* 23, 657–729.
- Tojo, K., Ikegawa, M., Maeda, N., Machida, S., Shiibayashi, M., Uchikawa, N., 1986. Computer modeling of scroll compressor with self adjusting back-pressure mechanism. In: 1986 International Compressor Engineering Conference at Purdue University.
- Tseng, C.-H., Chang, Y.-C., 2006. Family design of scroll compressors with optimization. *Applied Thermal Engineering* 26, 1074–1086.
- Wassgren, C., 2009. ME 510 Gas Dynamics Class Notes (Purdue University). Boiler Copy Maker.
- Yanagisawa, T., Shimizu, T., 1985. Leakage losses with a rolling piston type rotary compressor. II. Leakage losses through clearances on rolling piston faces. *International Journal of Refrigeration* 8 (3), 152 – 158.
- Youn, Y., Cho, N.-K., Lee, B.-C., Min, M.-K., 2000. The characteristics of tip leakage in scroll compressors for air conditioners. In: 2000 International Compressor Engineering Conference at Purdue University.
- Yuan, X., Chen, Z., Fan, Z., 1992. Calculating model and experimental investigation of gas leakage. In: 1992 International Compressor Engineering Conference at Purdue University.